American Journal of Pathology, Vol. 163, No. 5, November 2003

Animal Model

A Golden Hamster Model for Human Acute Nipah Virus Infection

K. Thong Wong,* Isabelle Grosjean,† Christine Brisson,‡ Barissa Blanquier,§ Michelle Fevre-Montange,‡ Arlette Bernard,‡ Philippe Loth,† Marie-Claude Georges-Courbot,† Michelle Chevallier,¶ Hideo Akaoka,‡ Philippe Marianneau,† Sai Kit Lam,* T. Fabian Wild,§ and Vincent Deubel†

From the Faculty of Medicine, University of Malaya, Kuala Lumpur, Malaysia; Unité de Biologie des Infections Virales Emergentes,† Institut Pasteur, Centre de Recherche Mérieux-Pasteur, Lyon, France; INSERM U.433,‡ Lyon, France; INSERM U.404,§ Centre d'Etudes et de Recherche en Virologie et Immunologie, Lyon, France; and the Laboratoire Marcel Mérieux,¶ Lyon, France*

A predominantly pig-to-human zoonotic infection caused by the novel Nipah virus emerged recently to cause severe morbidity and mortality in both animals and man. Human autopsy studies showed the pathogenesis to be related to systemic vasculitis that led to widespread thrombotic occlusion and microinfarction in most major organs especially in the central nervous system. There was also evidence of extravascular parenchymal infection, particularly near damaged vessels (Wong KT, Shieh WJ, Kumar S, Norain K, Abdullah W, Guarner J, Goldsmith CS, Chua KB, Lam SK, Tan CT, Goh KJ, Chong HT, Jusoh R, Rollin PE, Ksiazek TG, Zaki SR, Nipah Virus Pathology Working Group: Nipah virus infection: Pathology and pathogenesis of an emerging paramyxoviral zoonosis. Am J Pathol 2002, 161:2153–2167). We describe here a golden hamster (*Mesocricetus auratus*) model that appears to reproduce the pathology and pathogenesis of acute human Nipah infection. Hamsters infected by intranasal or intraperitoneal routes died within 9 to 29 days or 5 to 9 days, respectively. Pathological lesions were most severe and extensive in the hamster brain. Vasculitis, thrombosis, and more rarely, multinucleated endothelial syncytia, were found in blood vessels of multiple organs. Viral antigen and RNA were localized in both vascular and extravascular tissues including neurons, lung, kidney, and spleen, as demonstrated by immunohistochemistry and *in situ* hybridization, respectively. Paramyxoviral-type nucleocapsids were identified in neurons and in vessel walls. At the terminal stage of infection, virus and/or viral RNA could be recovered from most solid organs and urine, but not from serum. The golden hamster is proposed as a suitable model for further studies including pathogenesis studies, anti-viral drug testing, and vaccine development against acute Nipah infection. *(Am J Pathol 2003, 163:2127–2137)*

A recent outbreak of a novel paramyxovirus subsequently named Nipah virus (NiV) infected hundreds of patients in Malaysia causing severe morbidity and a mortality rate of ~40%.[1–3] Patients developed symptoms ranging from fever and headache to a severe acute febrile encephalitic syndrome. Although the majority of symptomatic patients who survived the acute infection eventually recovered without serious sequelae, a small number were readmitted with relapsed encephalitis months and years later.[4] The clinical features and pathogenesis of relapsed encephalitis were found to be distinct from acute NiV encephalitis. Pig-to-human transmission through close contact is now well established, with the pig playing the part of an amplifying host for the virus.[5–8] The natural host is very likely to be the fruit bat because NiV has been isolated from bat's urine.[9] Thus, the NiV outbreak represents the most serious viral zoonosis that has emerged from bats recently.[10]

Based on studies of NiV-infected human tissues, the pathology and pathogenesis of NiV infection is beginning to be understood.[1,2,11,12] In acute NiV infection present evidence suggests that after primary viral replication, viremia occurred spreading the virus systemically. Blood vessels became infected resulting in widespread vasculitis, which led to thrombosis, vascular occlusion, isch-

Supported by a Pasteur Institute (Cantarini) fellowship and a travel grant from the French Embassy, Malaysia (to K. T. W.); the Malaysian Government (IRPA grants 06-02-03-0741, 06-02-03-0743, and 06-02-03-0744); and by the Délégation Générale de l'Armement (grant no. 01.34.027.00.470.75.01).

Accepted for publication July 29, 2003.

Address reprint requests to Dr. K. Thong Wong, Department of Pathology, Faculty of Medicine, University of Malaya, 50603 Kuala Lumpur, Malaysia. E-mail: wongkt@um.edu.my.

emia, and/or microinfarction in multiple organs, affecting the central nervous system (CNS) most severely.[1,2,11,12] Extravascular parenchymal tissues, most notably neurons, were also susceptible to infection. It has been postulated that a combination of CNS ischemia and/or microinfarction and direct neuronal infection may contribute to the severe neurological manifestations seen in acute NiV infection.[12]

Attempts to further understand the early pathogenesis of acute NiV infection were hampered by the lack of an animal model. Present knowledge of the pathology and pathogenesis of acute NiV infection relates to the late stages of the disease because the studies were based on human autopsies. Naturally and experimentally infected animals including pigs and cats that have been studied so far showed vasculitis but not the typical encephalitis found in human NiV infection, and thus may not be suitable as models.[13] The anti-viral ribavirin, which was used as an empirical therapy in infected patients and reported to be effective, has yet to be fully evaluated in animal experiments.[14] Likewise, other anti-viral agents and newly-developed vaccines could not be tested for their potential usefulness in NiV infection because of the lack of a good model. Controlled transmission studies in animal models could be conducted to investigate viral infectivity and the routes of infection.

In this study we investigated several animal species as potential models for acute NiV infection, and identified the golden hamster (*M. auratus*) as a suitable model. The pathological lesions in hamsters infected intranasally and intraperitoneally were characterized by various approaches, and showed a high degree of similarity to those found in the human disease. We also attempted to correlate virus isolation and viral genome detection in various infected organs with pathological changes found therein.

Materials and Methods

Virus Stock and Titration

NiV isolated from a patient's cerebrospinal fluid was received in the Jean Mérieux Laboratory in Lyon, France, from Dr. K. B. Chua and Dr. S. K. Lam (University of Malaya, Kuala Lumpur, Malaysia) after two passages in Vero cells. Virus stock was obtained after a third passage on Vero cells conducted under biosafety level 4 (BSL-4) containment.

After 1 to 2 days when Vero cells showed fusion and syncytia formation, the supernatant was harvested for virus. Virus stock was titrated in 6-well plates by incubating 200 μl of serial 10 times dilution of supernatant in each well (containing 10^6 Vero cells per well) for 1 hour at 37°C. The cells in each well were washed twice with Dulbecco's minimum essential medium, and 2 ml of 1.6% carboxymethylcellulose in Dulbecco's minimum essential medium containing 2% fetal calf serum were added to each well. After incubation for 5 days at 37°C, and the wells were washed with phosphate-buffered saline (PBS), pH 7.4, fixed with 10% formalin for 20 minutes, washed, and stained with methylene blue. The virus titer in the supernatant after 24 hours of infection at a multiplicity of infection of 0.01 was 2×10^7 plaque-forming units (pfu)/ml.

Animal Infection Experiments

Altogether three sets of animal studies were done. In the first study, preliminary testing for susceptibility to NiV infection was done on two groups of animals comprising five mice, two guinea pigs and two hamsters each. Four-week-old, female Swiss mice (Charles River, L'Arbresle, France), 4-month-old, male Hartley guinea pigs (Charles River), and 2-month-old male golden hamsters (Janvier, Le Fenest St. Isle, France) were used in this experiment in which each group was inoculated either by the intranasal (IN) or the intraperitoneal (IP) route. For the IN route, 30 μl of virus stock (6×10^5 pfu) was given to each animal, whereas for the IP route 0.5 ml (10^7 pfu) was inoculated. The animals were housed in ventilated containment equipped with Hepa filters in the BSL-4 lab, and observed for signs of infection. We followed the French regulations for handling of animals and the strict procedures imposed for work in high-security BSL-4 containment.

Based on the results of the first study, a second study was then performed on adult hamsters (7 to 14 weeks old) using IN and IP inoculation routes to determine the lethal doses needed to kill 50% of the animals (LD_{50}). Groups of six hamsters were infected with 10-fold dilutions of NiV stock and observed twice daily throughout 4 weeks. The mice and guinea pigs from the first study were not studied further.

To investigate the possibility of on-going reinfection between animals housed together in the same cage contributing to mortality, a third study was done. In this study two hamsters infected by IP route with 10^5 pfu of virus were placed 3 days after inoculation in the same cage as four uninfected hamsters. The animals were observed and blood samples obtained for serology after 30 days.

Suitable tissue specimens from the first and second studies including blood, brain, lung, heart, liver, spinal cord, spleen, and kidney were collected from a total of 12 hamsters who died recently ($\leq$12 hours) or were terminally moribund. The latter were anesthetized with ketamine and xylazine, and exsanguinated by cardiac puncture and necropsied. Urine was collected from the bladder whenever possible. Animals discovered dead after more than 12 hours were not studied.

Tissues were frozen at −80°C for viral culture in the BSL-4 lab and reverse transcriptase-polymerase chain reaction (RT-PCR) analysis. For histopathological studies, tissues were fixed in 10% buffered formalin for at least 15 days before routine tissue processing and paraffin embedding outside the BSL-4 laboratory. Tissues from the nasal passage and cervical lymph nodes were also dissected out from formalin-fixed carcasses for routine processing and paraffin embedding only.

For electron microscopy, fresh or formalin-fixed tissues were fixed in 3% glutaraldehyde in 0.1 mol/L of phosphate buffer, pH 7.4, for a few hours and transferred to phosphate buffer. Similarly, tissues for immunoelectron microscopy were fixed in 2% paraformaldehyde/0.05%

glutaraldehyde, and transferred to buffer. In addition, electron microscopy and immunoelectron microscopy tissues that were initially not formalin fixed were γ-irradiated (2×10^6 rads) to further ensure noninfectivity.

Blood samples were collected by cardiac puncture at necropsy or obtained from the retroorbital sinus in surviving animals. The NiV doses causing mortality of 50% of the hamsters were calculated based on the method of Reed and Muench.[15]

Virus Isolation and Titration

The quantity of infectious virus particles was measured in urine and other tissues by plaque titration in Vero cells in the BSL-4 lab. A small fragment of tissue was mechanically crushed (Minibeadbeater; Biospec, Bartlesville, OK) twice for 30 seconds each in a 2-ml tube containing 0.5 ml of sterile glass beads and 0.5 ml of Dulbecco's minimum essential medium, and centrifuged at 3000 rpm for 5 minutes at 4°C. The supernatant was cultured for virus as described above.

Nipah Antibody Testing

Sera of infected hamsters were tested individually by enzyme-linked immunosorbent assay for NiV antibodies. Crude extracts of NiV antigens were prepared from infected Vero cells at an multiplicity of infection of 0.01 pfu/cell for 24 hours. The cells were washed with PBS and lysed in PBS containing 1% Triton X-100 (10^7 cells/ml) at 4°C for 10 minutes. The cell lysate was sonicated twice for 30 seconds each to full cell destruction and centrifuged at 5000 rpm at 4°C for 10 minutes. The supernatant was frozen at −80°C. Noninfected Vero cells were similarly treated to prepare an antigen control. Cross-titration of the NiV antigens was performed with serum from a convalescent, NiV-infected patient to determine the antigen titer corresponding to the dilution showing the highest OD reading.

RT-PCR

Total RNA was extracted from 20 μl of serum and urine and from mechanically crushed, fresh-frozen tissues using an RNA extraction kit (QIAamp Viral RNA Mini Kit; Qiagen Inc., Valencia, CA). After the lysis step, the rest of the extraction protocol was performed outside the BSL-4 lab. Approximately 2 μg of the extract was used in a RT-PCR protocol (Titan One Tube RT-PCR System; Roche Diagnostics, Mannheim, Germany) to detect the NiV nucleoprotein (N) gene. Previously published, specific primers used,[1] and the reaction conditions are shown in Table 1.

Light Microscopy

Formalin-fixed, paraffin-embedded tissues were microtomed 3 μm thick, placed on glass slides, and stained with hemalin-phloxine-safranin stain for light microscopy.

Table 1. Nipah Virus Nucleoprotein Gene Specific Primers and RT-PCR Conditions

Primers	
5′-CTGCTGCAGTTCAGGAAACATCAG-3′	
5′-ACCGGATGTGCTCACAGAACTG-3′	
RT-PCR mix	
Primers (10 pmol/μl)	5 μl each
dNTP (10 mmol/L)	4 μl
Buffer (5×)	10 μl
DTT (100 mmol/L)	2 μl
RNAse inhibitor (5 U/μl)	1 μl
Titan enzyme mix	1 μl
RNA template	10 to 20 μl
H_2O to final volume of 50 μl	
RT-PCR conditions	
50°C	30 min
94°C	5 min
94°C	1 min × 30 cycles
50°C	1 min × 30 cycles
72°C	2 min × 30 cycles
72°C	10 min
4°C	Hold

Immunohistochemistry (IHC)

Tissue sections, 3 μm in thickness, were placed on silanized slides and dewaxed by xylene and graded ethanol washes. Antigen was retrieved by thermic treatment in pH 6.0 citrate buffer at 96 to 98°C for 40 minutes. The modified IHC procedure was based on a previously described method and done at room temperature (20°C) throughout.[12] Briefly, sequential steps included 1) background blocking; 2) rabbit polyclonal anti-NiV antibody, 1:500, 1 hour; and 3) biotinylated, goat anti-rabbit secondary antibody, and horseradish peroxidase-linked streptavidin and diaminobenzidine substrate according to the manufacturer's protocol (DAKO, Trappes, France). The slides were counterstained in hematoxylin and mounted.

In Situ *Hybridization*

For *in situ* hybridization, digoxigenin-labeled riboprobes were generated from the 228-bp, RT-PCR product using the primers in Table 1. This fragment was cloned in the pdrive-cloning vector (Qiagen PCR cloning kit, Qiagen Inc.) according to the manufacturer's protocol. Plasmids containing the correct insert in both orientations were linearized with the restriction endonuclease *Hin*dIII, and transcribed to produce sense and anti-sense riboprobes using the DIG RNA labeling kit (Roche Diagnostics). The riboprobes were treated with DNase (15 minutes, 37°C) then purified by ethanol precipitation before use.

The *in situ* hybridization method was slightly modified from a previous method.[16] Briefly, dewaxed tissue sections were pretreated with HCl followed by 0.1 mg/ml of proteinase K in 100 mmol/L Tris/50 mmol/L ethylenediaminetetraacetic acid, pH 8.0 buffer (15 minutes, 37°C), followed by two PBS washes. Washes with glycine and prehydridization steps were omitted. The slides were incubated overnight at 45°C in a moist chamber (Hybaid Omnislide, National Labnet Co., Woodbridge, NJ) with 1:50 to 1:100 dilution of riboprobes in standard filtered hybridization solution as described.[16]

Posthybridization steps included sequential washings with decreasing concentrations of sodium chloride/sodium citrate and Tris buffers as described previously.[17] The slides were then incubated with alkaline phosphatase-conjugated, anti-digoxigenin Fab fragments (Roche Diagnostics) diluted 1:1000, followed by various buffers and NBT/BCIP solution (Roche Diagnostics) according to manufacturer's protocol. The color reaction was stopped after ~45 minutes. The slides were counterstained with hematoxylin and coverslipped in an aqueous medium.

Electron Microscopy and Immunoelectron Microscopy

Formalin- or glutaraldehyde-fixed tissues were postfixed, dehydrated, and embedded in Epon (Ladd, UK) as described, and ultra-thin sections (70 nm) were counterstained with uranyl acetate and lead citrate.[18] Slides were examined on a TEM Jeol 1200 EX electron microscope.

Immunogold staining was performed on paraformaldehyde/glutaraldehyde-fixed tissue embedded in LR White (Inland, France) with omission of the osmium tetroxide postfixation step. Ultra-thin sections on 200-mesh nickel grids (Oxford Instruments, France) were incubated in 20 mmol/L Tris, pH 7.4/150 mmol/L NaCl (TBS) containing 1% albumin for the blocking step, then in TBS-0.1% albumin for the incubation with primary antibody. The linking secondary antibody was coupled with 10-nm colloidal gold (Biocell Tebu, France) and the sections were counterstained with uranyl acetate and examined under 60 KV.

Results

Animal Infection Experiments: Survival and LD_{50}

In the first study, none of the Swiss mice inoculated by either the IN or IP route developed any clinical signs. Only Hartley guinea pigs that were infected by IP route, and therefore received 10^7 infectious viral particles, showed transient fever and weight loss after 5 to 7 days but they recovered. Golden hamsters infected by both routes showed difficulties with movement and balance, and rapidly died 5 to 8 days after infection.

Figure 1 shows the dose-survival graphs of hamsters in the second study that were inoculated with serial dilutions of viruses, namely 1 to 10^4 pfu by IP route and 10 to 10^6 pfu by IN route. The time interval between infection and appearance of clinical signs and death were shorter in IP-infected hamsters. They died 5 to 9 days after infection and <24 hours after the appearance of tremor and limb paralysis. Conversely, the majority of IN-inoculated animals showed a progressive deterioration presenting with imbalance, limb paralysis, lethargy, muscle twitching, and breathing difficulties in the final stages. The majority of animals died between 9 and 15 days. However, six animals died later, one at day 18, two at day 21 and three at day 29. The LD_{50} of animals by IP and IN route was, respectively, 270 pfu and 47,000 pfu for each animal.

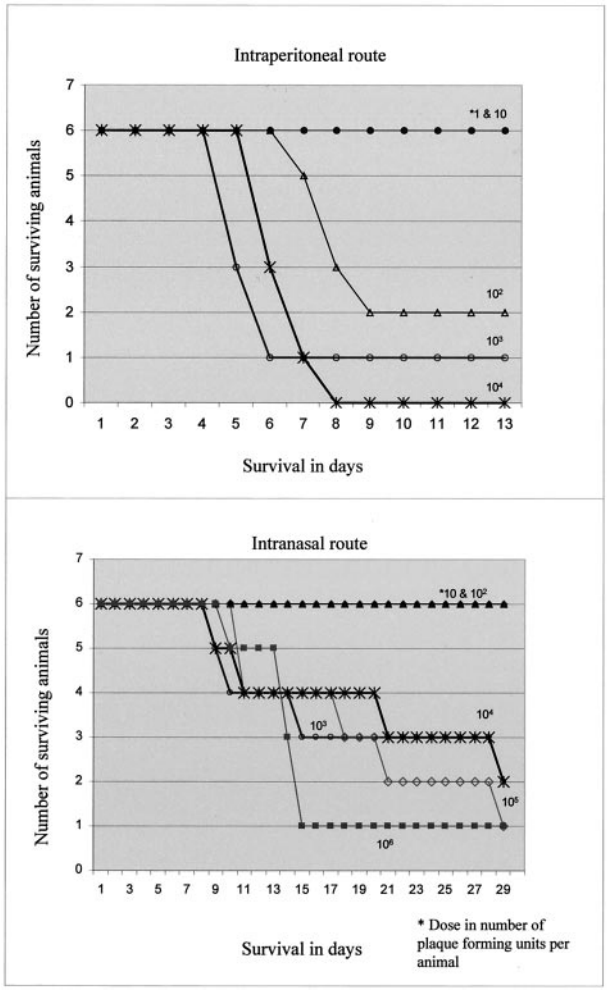

Figure 1. Survival graphs of hamsters infected by NiV via different routes and doses.

In animals surviving more than 30 days after infection, and that were inoculated with lower viral doses (1 and 10 pfu/animal for IP route; 10 and 10^2 pfu/animal for IN route) there was no seroconversion (data not shown). In fact, none of these animals died or showed any signs of illness. In contrast, surviving animals infected with higher viral doses, and that were kept in the same cages as animals given the same doses and died, had high levels of antibody (data not shown). Nonetheless, these survivors showed no clinical signs of illness.

In the transmission study (third study) in which uninfected animals were housed together with infected animals, none of the uninfected animals showed evidence of disease or seroconversion (data not shown).

Viral Isolation and Viral Genome Detection

In general, RT-PCR of various animal specimens taken at autopsy showed that NiV viral genome could be detected in most tissues and urine (Table 2). Serum was the notable exception in that it was uniformly negative for viral genome. Because of this, viral culture was not attempted on serum. Where both these tests were performed, the

Table 2. RT-PCR Analysis, Nipah Virus Culture, and Pathological Lesions in Infected Hamster Specimens

Tissue/specimen	No. of animals with pathological lesions/total no. of animals (%)	No. of positive animals/total no. of animals (%)			
		Intranasal route*		Intraperitoneal route	
		RT-PCR	Virus culture	RT-PCR	Virus culture
Blood	na†	0/5 (0%)	nd‡	0/2 (0%)	nd
Urine	na	3/3 (100%)	0/2 (0%)	2/3 (67%)	1/1 (100%)
Brain	8/12 (67%)	4/5 (80%)	1/5 (20%)	3/3 (100%)	2/3 (67%)
Spinal cord	0/7 (0%)	na	na	3/3 (100%)	2/2 (100%)
Lung	4/12 (33%)	4/5 (80%)	0/5 (0%)	3/3 (100%)	2/3 (67%)
Kidney	2/12 (17%)	4/5 (80%)	1/5 (20%)	3/3 (100%)	2/3 (67%)
Spleen	1/12 (8%)	5/5 (100%)	0/5 (0%)	3/3 (100%)	1/3 (33%)
Liver	4/12 (33%)	5/5 (100%)	0/5 (0%)	3/3 (100%)	2/3 (67%)
Heart	3/12 (25%)	3/5 (60%)	0/5 (0%)	3/3 (100%)	0/3 (0%)

*The LD_{50} of animals by intranasal and intraperitoneal routes was respectively 47,000 and 270 plaque forming units for each animal.
†na = tissues not available or not suitable for analysis.
‡nd = tissues available but analysis not done because RT-PCR is negative.

range of tissues positive for viral culture correlated well with RT-PCR, although the percentage for positivity was lower for viral culture especially in intranasally infected hamsters.

Pathological Features

Blood Vessels

Vascular pathology was found in multiple organs including brain, lung, liver, kidney, and heart. In large blood vessels the more florid changes were characterized by focal, transmural fibrinoid necrosis with surrounding inflammation (Figure 2A). However, vasculitis may be more subtle with fewer inflammatory cells (Figure 2E and Figure 3A), and very focal nuclear pyknosis and karyorrhexis (Figure 2E). Multinucleated syncytia arising from the endothelium were encountered in one hamster that died 8 days after intraperitoneal inoculation (Figure 2, C and D). Thrombosis could be found in the lumen of some vessels (Figure 4B). Viral antigen and genome as demonstrated by IHC and *in situ* hybridization, respectively, localized to endothelial cells and syncytia, and underlying smooth muscle of the tunica media in blood vessels (Figure 2, D and F). Viral nucleocapsids were detected in the blood vessel wall.

CNS

The brain was the most severely affected in terms of vascular and parenchymal lesions compared with other organs (Table 2). Apart from vasculitis, the most striking features were in the neurons usually found in the vicinity of vasculitis. Affected neurons showed numerous eosinophilic inclusion bodies in the cytoplasm (Figure 3C). These inclusions, as well as neuronal cytoplasm with no obvious inclusions, and neuronal processes, were often positive for both viral antigen and RNA (Figure 3; D to F). Ultrastructurally, these inclusions were composed of defined masses of filamentous nucleocapsids of the fuzzy type typically associated with paramyxoviruses (Figure 5A). These inclusions were immunolabeled by NiV-specific antibodies (Figure 5B). Nuclear inclusions could not be found but there was evidence of nuclear IHC positivity (Figure 3D, inset).

Other parenchymal changes included focal areas with evidence of ischemia/infarction and edema (Figure 3B). Parenchymal and meningeal inflammation were generally mild, and only occasionally were perivascular cuffing and neuronophagia observed. Rarely, IHC positivity was noted in ependymal lining (Figure 3E), and in mononuclear cells found in the meninges and choroid plexus. The choroid plexus lining epithelium however was negative for viral antigen and genome. IHC and *in situ* hybridization positivity was not observed in the white matter.

Other Organs

In the lung, small discrete nodular or more confluent areas of parenchymal inflammation, often associated with vasculitic vessels, could sometimes be observed (Figure 4, A and B). Inflammatory cells consisted mainly of a varying mixture of macrophages, neutrophils and lymphocytes. Multinucleated giant cells and inflammatory cells positive for NiV by IHC and *in situ* hybridization were rare. Fibrinoid necrosis of lung parenchyma was rare and focal. Bronchitis, multinucleated syncytia, or other evidence of NiV infection of bronchial epithelium were not found.

Glomerular lesions in the kidney were rare but the most florid lesions had thrombotic plugs in the glomerular capillaries, peripheral multinucleated syncytia, and surrounding inflammation (Figure 4C). Viral antigen was detected only in the occasional glomerulus and tubule (Figure 4D). In the kidney of several animals, the covering epithelium of the renal papilla that project into the calyces, consistently demonstrated the presence of viral antigen (Figure 4E) but *in situ* hybridization was negative in the same epithelium.

The rare focus of necrosis was noted in the spleen but no vasculitis or multinucleated giant cells were observed. IHC and *in situ* hybridization were occasionally positive in periarteriolar lymphoid cells (Figure 4F). There appeared to be no specific liver parenchymal lesions. In the heart, myocarditis associated with infarction was only rarely observed (Figure 2B). No inflammation or viral antigen was detected in lymph nodes or nasal epithelium.

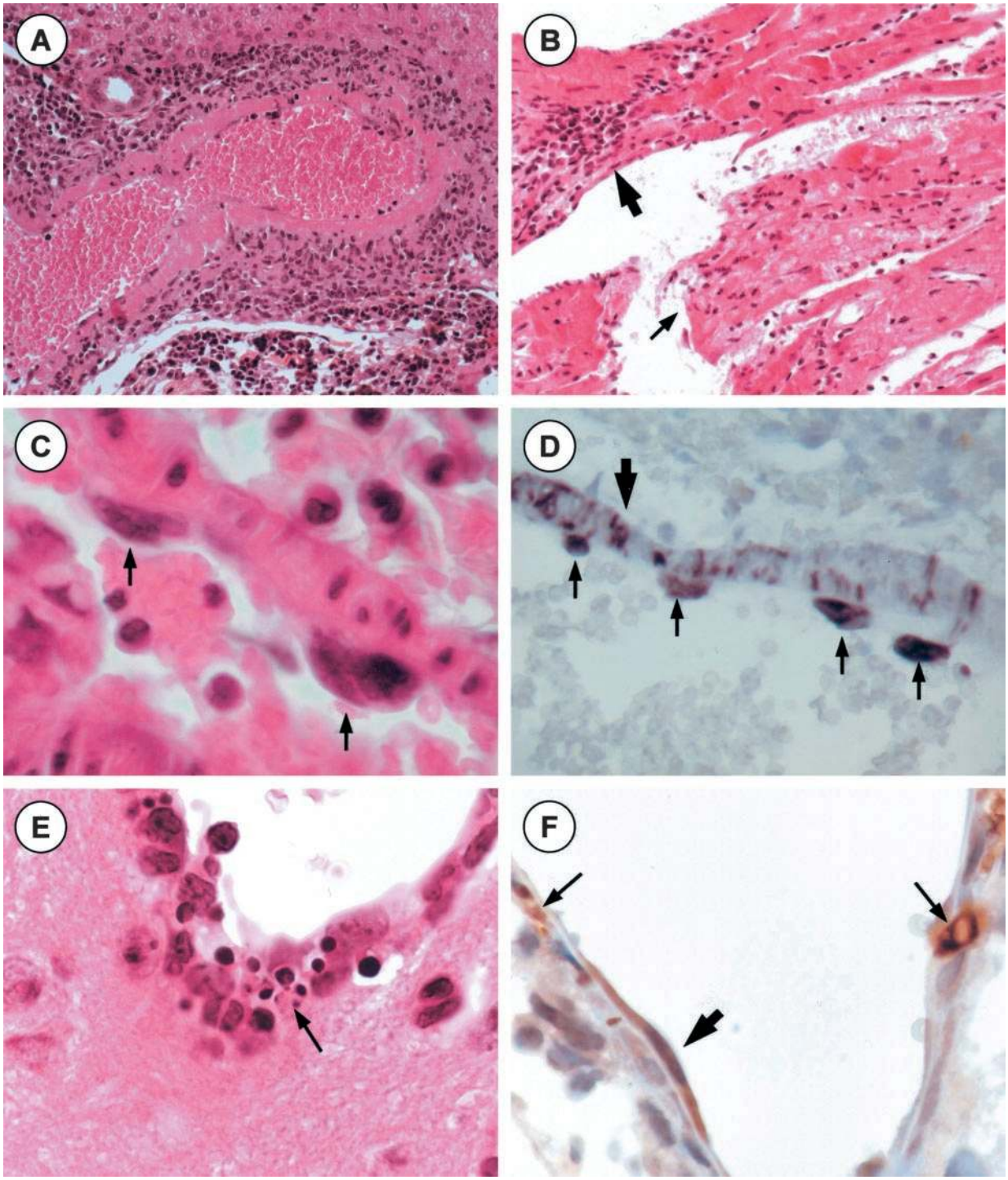

Figure 2. Vascular and parenchymal pathology in acute Nipah infection. **A:** Large artery in liver showing focal, transmural fibrinoid necrosis with surrounding inflammation. **B:** Myocardial necrosis (**thin arrow**) with adjacent inflammation (**thick arrow**). **C:** Multiple endothelial multinucleated syncytium (**arrows**) in pulmonary artery. **D:** Viral RNA was demonstrated in endothelial syncytia (**thin arrows**) and vascular smooth muscle (**thick arrow**) in the same lung. **E:** Necrosis and karyorrhexis in a cerebral vessel. **F:** Viral antigen localized to endothelium (**thick arrow**) and smooth muscle (**thin arrows**) in a meningeal blood vessel. **A–C**, **E:** Hemalin-phloxine-safranin stain; **D:** *in situ* hybridization, hematoxylin counterstain; **F:** IHC, hematoxylin counterstain. Original magnifications: ×20 (**A**, **B**); ×40 (**D**); ×100 (**C**, **E**, **F**).

Intraperitoneal versus *Intranasal Inoculation*

In general, the spectrum and severity of pathological lesions in the blood vessels and the other organs showed no significant difference between IP- and IN-inoculated animals.

Discussion

Of the three animal species, mouse, guinea pig, and hamster, that were inoculated with NiV, the hamster appeared to be the most susceptible. Depending on the route and dose most of the infected hamsters developed

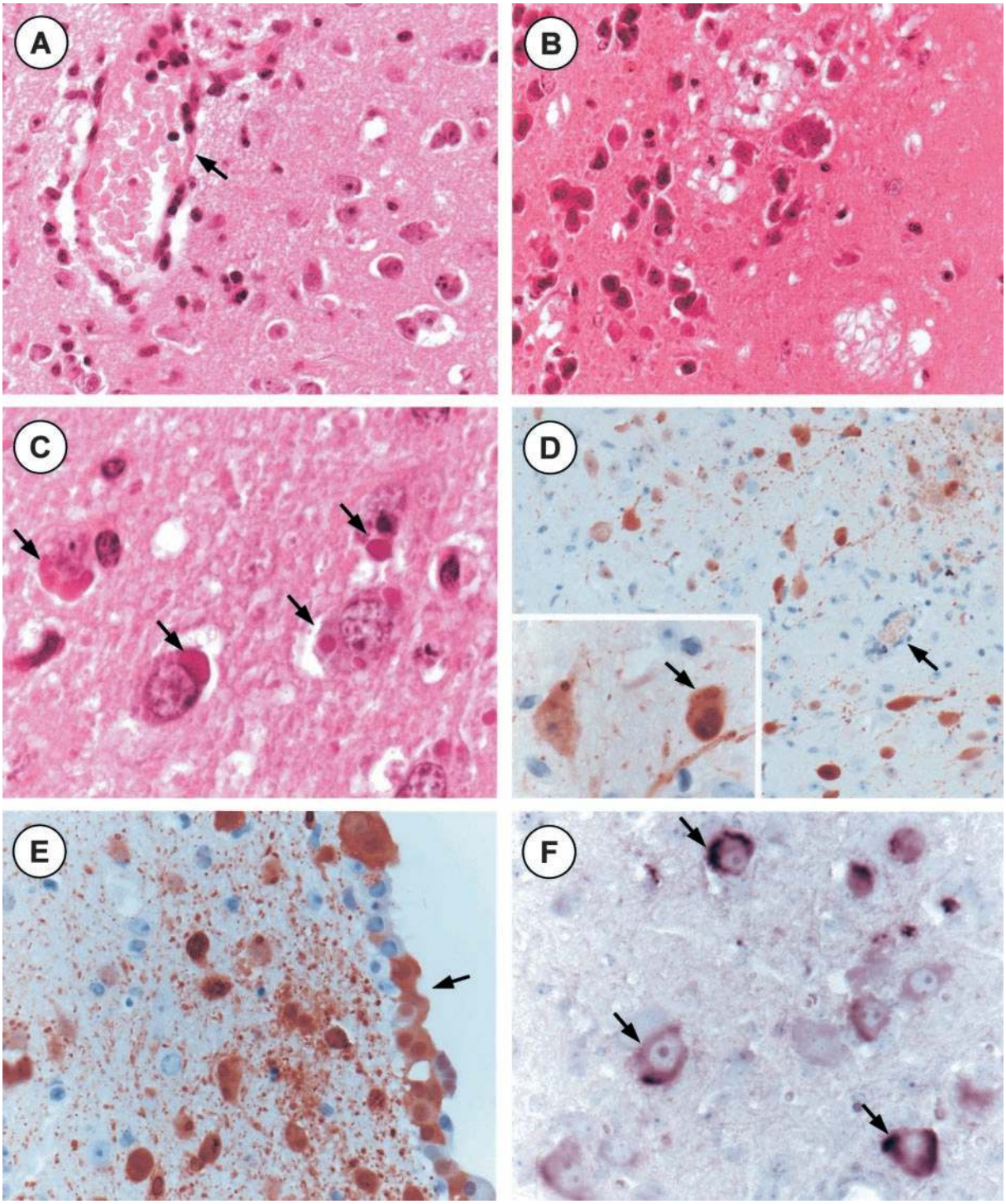

Figure 3. Cerebral pathology in acute Nipah infection. **A:** Small vessel vasculitis (**arrow**) characterized by mild inflammation in the vicinity of infected neurons. **B:** Focal areas of parenchymal ischemia, infarction, and edema. **C:** Neurons with eosinophilic viral inclusions (**arrows**). **D**: Immunolocalization of viral antigens to neurons in the nucleus (**inset**, **arrow**), cytoplasm, and processes near a vasculitic vessel (**arrow**). **E:** Viral antigens localized to ependymal lining (**arrow**) and neurons. **F:** Neurons demonstrating viral RNA in the cytoplasm (**arrows**). **A–C:** Hemalin-phloxine-safranin stain; **D**, **E:** IHC, hematoxylin counterstain; **F:** *in situ* hybridization, hematoxylin counterstain. Original magnifications: ×40 (**A**, **B**, **E**, **D** (**inset**), ×20 (**D**); ×100 (**C**, **F**).

severe illness. Studies of tissues obtained from infected hamsters suggested that it is a suitable animal model for acute NiV infection, demonstrating most of the characteristics found in human acute NiV infection.

Hamsters could be infected by either IP or IN routes but infection by the IP appeared to kill animals faster than the IN route. Furthermore, far lower IP doses were required to kill the same number of animals as shown by the widely disparate LD_{50} doses between IP- and IN-infected animals. This is probably not surprising because IN-inoculated NiV presumably had to penetrate the mucosal barrier of the aerodigestive tract before infection could

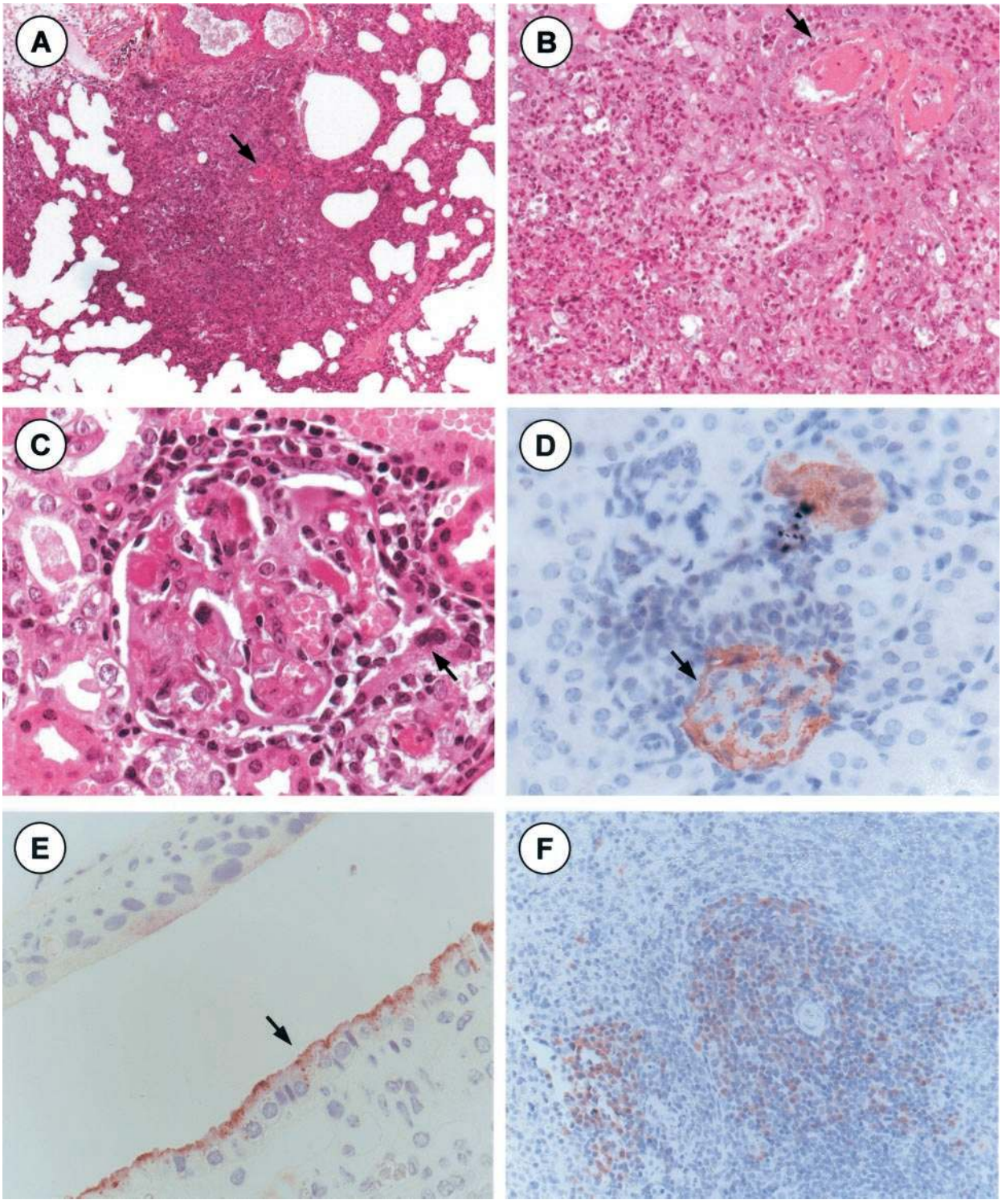

Figure 4. A, **B:** Inflammation in the lung parenchyma associated with vasculitic and thrombotic blood vessels (**arrow**). **C:** Glomerulitis characterized by thrombotic plugs, inflammation, and syncytial formation (**arrow**) at the periphery of the glomerulus. **D:** Viral antigens were detected in a tubule and glomerulus (**arrow**). **E:** Viral antigens found in the epithelium covering the papilla in the kidney (**arrow**). **F:** Viral antigens demonstrated in lymphoid cells of the white pulp in the spleen. **A–C:** Hemalin-phloxine-safranin stain; **D-F:** IHC, hematoxylin counterstain. Original magnifications: ×5 (**A**); ×20 (**B**, **F**); ×40 (**C–E**).

take place, whereas IP-inoculated NiV theoretically could enter the systemic circulation directly. Interestingly, the absence of detectable antibodies in the sera of animals surviving more than 30 days after infection, and that were either IP-inoculated with ≤10 pfu/animal or IN-inoculated with $\leq 10^2$ pfu/animal, suggested that these animals could not be infected with these low doses.

Histopathological studies of infected hamster tissues showed that blood vessels, particularly those in the CNS, developed vasculitis characterized by necrosis and in-

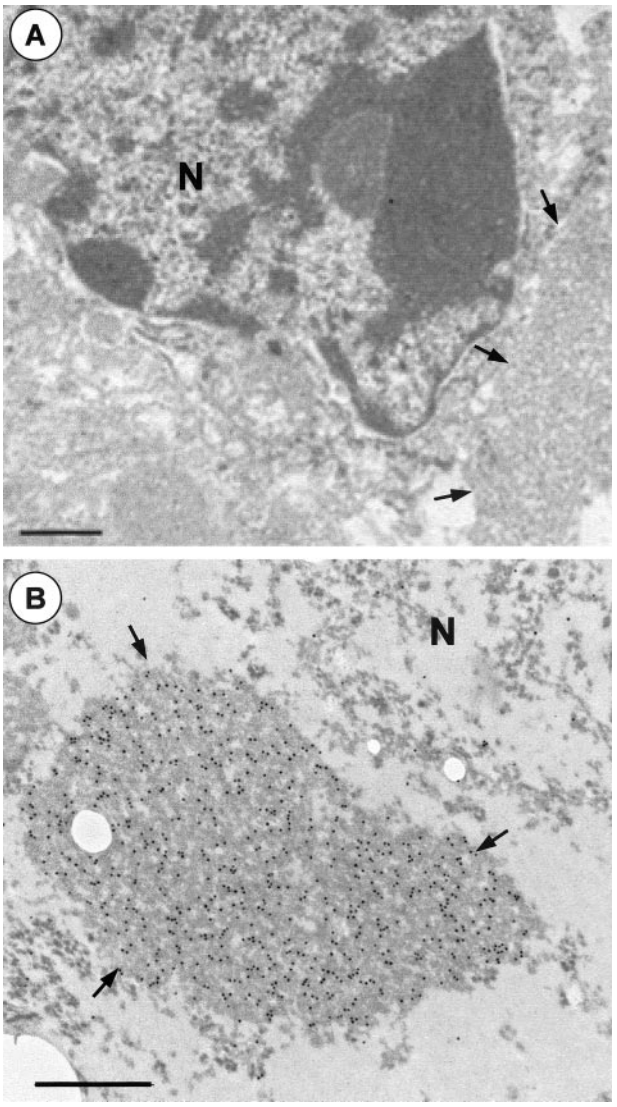

Figure 5. A: Cytoplasmic viral inclusion (**arrows**) composed of nucleocapsids in a neuron. **B:** Immunogold-labeled neuronal viral inclusion (**arrows**) demonstrated by immunoelectron microscopy with specific anti-Nipah antibody. *N*, nucleus. Scale bars, 0.5 μm.

tramural inflammation. Evidence of direct viral infection of the vessel wall, including the endothelium and smooth muscle, was provided by the presence of endothelial multinucleated syncytia formation, and the detection of viral nucleocapsid, antigen, and genome in the vascular wall. Most likely as a result of vasculitis, thrombosis and vascular obstruction occurred producing distal ischemia and microinfarction in the brain, lung, and heart. Blood vessels in the kidney were also involved with vasculitis although to a lesser extent. These findings are similar to those found in human infection.[12] A notable exception could be vasculitis in the liver, which was not reported in human infection.

In addition to ischemia and infarction, neurons in the brain were also infected as evidenced by neuronal viral inclusions, antigen, and genome. Viral inclusions found mainly in the cytoplasm consisted of typical paramyxoviral-type nucleocapsids, which were confirmed to be NiV nucleocapsids by immunoelectron microscopy. The findings in blood vessels, parenchyma, and neurons of the brain makes it the major target in acute NiV infection, and this is borne out by the fact that sick animals had prominent CNS signs such as paralysis and gait and balance abnormalities. In the case of human infection, the CNS symptoms and signs were very prominent and the CNS was also the most severely affected organ.[3,12]

Evidence of extravascular tissue infection was noted in non-CNS organs although to a much lesser extent. In the lung, in inflamed areas adjacent to vasculitic blood vessels, occasional inflammatory cells showed the presence of viral antigen and genome. In contrast to the infected human lung where parenchymal fibrinoid necrosis was commonly encountered, this feature was rare in the infected hamster.[12] The nodular inflamed areas adjacent to vasculitis in hamster lung could be necrotic areas that subsequently became inflamed.

In the hamster kidney the vasculitis and glomerular lesions resembled those reported in humans.[2,12] The consistent presence of viral antigen but not of viral genome in the covering epithelium of the renal papilla suggests possible reabsorption of IHC-detectable viral proteins leaked into the urine. Williamson and colleagues,[19] found evidence of urothelial infection in the urinary bladder of Hendra virus-infected guinea pigs but there was no information on epithelial infection in the kidney. The presence of viral antigen and genome in the periarteriolar lymphoid cells of the spleen suggests that active viral replication occurred there.

The limited published data on NiV-infected animals comprising observations on field and experimentally-infected pigs and cats, and field-infected dogs and horses, showed that systemic vasculitis was the common feature in all these animals.[13] However it appears that in none of these animals was encephalitis and neuronal infection as convincingly demonstrated, as in the hamsters in our study. In the case of the pig and cat, there was evidence of meningitis but no distinct encephalitis nor any apparent direct evidence of neuronal infection. In the dog and horse, apart from meningitis, focal brain parenchyma rarefaction was also found but there is no data on the presence, if any, of encephalitis or of direct neuronal infection. We have found that mice produced antibodies to NiV after repeated infection (unpublished observations), but in our experiment they did not appear to show clinical illness, and therefore were not studied further. Thus, present evidence suggested that the pig, cat, dog, horse, and mouse may not be good models for the acute human disease, which is typified by severe illness, prominent vasculitis, encephalitis, and direct neuronal infection.

Tissue localization of virus by IHC and *in situ* hybridization was confirmed by virus isolation and/or RT-PCR in all of the solid organs tested. Overall, RT-PCR was more sensitive than virus isolation as a confirmatory test for NiV infection in both IN- and IP-infected animals. The lower rate of virus isolation from IN-infected compared with IP-infected animals could be related to the longer survival of the former, which presumably favored effective immune clearance of virus from solid organs. However, RT-PCR was negative in serum in all seven animals

tested irrespective of survival duration suggesting that the immune system may be more efficient in clearing virus from the circulation or that viremia occurred early in the infection. Alternatively, viral particles may be transported inside infected blood leukocytes. Further studies in the hamster model will be needed to clarify this.

In previous human studies viremia was also postulated to have occurred, and to have occurred early based on the simultaneous involvement of multiple organs and disseminated blood vessels, and the observation that vascular lesions such as vasculitis, thrombosis, and infarction occurred earlier than extravascular parenchymal lesions.[12] Viremia appears to be corroborated by our data that also showed simultaneous and widespread organ involvement.

The presence of virus in urine as confirmed by RT-PCR and virus isolation correlates well with kidney glomerular injury. Virus excretion in human urine has been reported from patients and postulated as a possible means of viral transmission to health care workers.[20] Interestingly, urine viral excretion in hamsters by itself may not be sufficient to cause viral transmission as suggested by observations in the experiment in which uninfected hamsters kept together with infected animals for 30 days did not develop any positive serology.

Oral ingestion and/or aerosol inhalation of infected secretions is thought to be responsible for pig-to-human viral transmission.[5] The successful infection of hamsters by the IN route appear to support this. The primary viral replication site or sites for NiV before the onset of viremia are unknown. In the case of measles, another paramyxovirus, there is evidence that the lung and lymph nodes are the primary viral replication sites.[21] Theoretically, demonstration of viral infection in the bronchial epithelium of the IN-infected animals could provide some evidence that the lung is a possible site but this was not found in our study, nor was there any evidence of virus in the lymph nodes. One possibility is that primary viral replication is an early event and therefore may not be found in terminally ill animals.

NiV access into the CNS is thought to be facilitated by vascular wall damage in human infection.[12] Our findings strongly support this because infected neurons were often found in the vicinity of vasculitis. The possibility of direct CNS infection via the olfactory bulb in our model is not supported by our data, which did not show a predilection for the olfactory bulb or structures connected to it. Choroid plexus infection may allow virus to leak into the cerebrospinal fluid and thus spread the virus but we have not found strong evidence for this in our model. Similarly, in the human studies there was no evidence for choroid plexus involvement.[12] However, in the guinea pig model for Hendra virus infection, a virus most closely related to NiV, choroid plexus involvement was thought to be a possible mechanism for virus spread into the CNS.[19] Ependymal lining infection in both humans[12] and the hamster model could possibly allow virus to enter the cerebrospinal fluid and thus spread the virus further.

In the absence of effective drugs and vaccines against NiV, this highly pathogenic virus has been classified as a class 4 agent. Animal experiments strictly require BSL-4 lab facilities with trained personnel wearing airtight, pressurized suits, and following strict procedures. Because the hamsters excrete virus in their urine, even though no cross infection seemed to have occurred in the experiment in which infected and noninfected animals were housed in the same cage, handling of the animals and cages require caution. The cages themselves are maintained in laminar flow cabinets with negative pressure and ventilated through HEPA filters. Whenever cages were removed for experiments, each cage is covered by a filtered cap and placed on a table that has vertical and filtered laminar airflow.

The establishment of an animal model for acute NiV infection should open the way to a greater understanding of its pathogenesis particularly in relation to the early events because present knowledge of NiV is based mainly on the end-stage disease. Potential anti-NiV drugs and vaccines could also be tested for effectiveness in the model. A greater understanding of the immune response could enable us to investigate if NiV could cause immunosuppression, a phenomenon well known in measles infection.[21] An animal model for relapsed NiV encephalitis is still elusive but long-term follow-up of large numbers of infected hamsters that eventually recovered could yield some cases of relapsed encephalitis because the prevalence of human relapsed encephalitis is low.[4]

Acknowledgments

We thank Dr. K. B. Chua (International Medical University, Malaysia), for the gifts of NiV isolates and patient serum; Dr. P. Hooper (Commonwealth Scientific & Industrial Research Organisation, Geelong Australia) for the gift of anti-Nipah antibodies for IHC; Dr. C. Leculier and T. Vallet for their strong support in the maintenance and biosecurity in the Laboratoire P4 Jean Mérieux where this research was performed; and CeCIL (Laennec, Lyon, France) for the use of electron microscopic facilities.

References

1. Chua KB, Bellini WJ, Rota PA, Harcourt BH, Tamin A, Lam SK, Ksiazek TG, Rollin PE, Zaki SR, Shieh W-J, Goldsmith CS, Gubler DJ, Roehrig JT, Eaton B, Gould AR, Olson J, Field H, Daniels P, Ling AE, Peters CJ, Anderson LJ, Mahy BWJ: Nipah virus: a recently emergent deadly paramyxovirus. Science 2000, 288:1432–1435
2. Chua KB, Goh KJ, Wong KT, Adeeba K, Tan PSK, Ksiazek TG, Zaki SR, Paul G, Lam SK, Tan CT: Fatal encephalitis due to Nipah virus among pig-farmers in Malaysia. Lancet 1999, 354:1257–1259
3. Goh KJ, Tan CT, Chew NK, Tan PSK, Kamarulzaman A, Sarji SA, Wong KT, Abdullah BJ, Chua KW, Lam SK: Clinical features of Nipah virus encephalitis among pig farmers in Malaysia. N Engl J Med 2000, 342:1229–1235
4. Tan CT, Goh KJ, Wong KT, Sarji SA, Chua KB, Chew NK, Murugasu P, Loh YL, Chong HT, Tan KS, Thayaparan T, Kumar S, Jusoh MR: Relapse and late-onset Nipah encephalitis. Ann Neurol 2002, 51:703–708
5. Parashar UD, Sunn LM, Ong F, Mounts AW, Arif MT, Ksiazek TG, Kamaluddin MA, Mustafa AN, Kaur H, Ding LM, Othman G, Radzi HM, Kitsutani PT, Stockton PC, Arokiasamy J, Gary JHE, Anderson LJ: Case-control study of risk factors for human infection with the new zoonotic paramyxovirus, Nipah virus, during a 1998–1999 outbreak of severe encephalitis in Malaysia. J Infect Dis 2000, 181:1755–1759

6. Ali R, Mounts AW, Parashar UD, Sahani M, Lye MS, Isa MM, Balathevan K, Arif MT, Ksiazek TG: Nipah virus among military personnel involved in pig culling during an outbreak of encephalitis in Malaysia, 1998–1999. Emerg Infect Dis 2001, 7:759–761
7. Amal NM, Lye MS, Ksiazek TG, Kitsutani PT, Hanjeet KS, Kamaluddin MA, Ong F, Devi S, Stockton PC, Ghazali O, Zainab R, Taha MA: Risk factors for Nipah virus transmission, Port Dickson, Negeri Sembilan, Malaysia: results from a hospital-based case control study. Southeast Asian J Trop Med Public Health 2000, 31:301–306
8. Chew MH, Arguin PM, Shay DK, Goh KT, Rollin PE, Shieh WJ, Zaki SR, Rota PA, Ling AE, Ksiazek TG, Chew SK, Anderson LJ: Risk factors for Nipah virus infection among abattoir workers in Singapore. J Infect Dis 2000, 181:1760–1763
9. Chua KB, Koh CL, Hooi PS, Wee KF, Khong JH, Chua BH, Chan YP, Lim ME, Lam SK: Isolation of Nipah virus from Malaysian island flying-foxes. Microbes Infect 2002, 4:145–151
10. Eaton BT: Introduction to current focus on Hendra and Nipah viruses. Microbes Infect 2001, 3:277–278
11. Wong KT, Shieh WJ, Kumar S, Karim N, Guarner J, Abdullah W, Zaki S: Nipah encephalitis: pathology and pathogenesis of a new, emerging paramyxovirus infection. Proceedings of the XIVth International Congress of Neuropathology, Birmingham, United Kingdom. Brain Pathol 2000, 10:794–795
12. Wong KT, Shieh WJ, Kumar S, Norain K, Abdullah W, Guarner J, Goldsmith CS, Chua KB, Lam SK, Tan CT, Goh KJ, Chong HT, Jusoh R, Rollin PE, Ksiazek TG, Zaki SR, Nipah Virus Pathology Working Group: Nipah virus infection: pathology and pathogenesis of an emerging paramyxoviral zoonosis. Am J Pathol 2002, 161:2153–2167
13. Hooper P, Zaki S, Daniels P, Middleton D: Comparative pathology of the diseases caused by Hendra and Nipah viruses. Microbes Infect 2001, 3:315–322
14. Chong HT, Kamarulzaman A, Tan CT, Goh KJ, Thayaparan T, Kunjapan SR, Chew NK, Chua KB, Lam SK: Treatment of acute Nipah encephalitis with Ribavirin. Ann Neurol 2001, 49:810–813
15. Reed LJ, Muench H: A simple method for estimating fifty percent endpoints. Am J Trop Med Hyg 1938, 27:493–497
16. Killen H, O'Sullivan MA: Detection of dengue virus by in situ hybridization. J Virol Methods 1993, 41:135–146
17. Komminoth P: Detection of mRNA in tissue sections using DIG-labeled RNA and oligonucleotide probes. Nonradioactive in Situ Hybridization Application Manual. Edited by S Grunewald-Janho. Mannheim, Boehringer Mannheim, 1996, pp 126–135
18. Goldsmith CS, Whistler T, Rollin PE, Ksiazek TG, Rota PA, Bellini WJ, Daszak P, Wong KT, Shieh W-J, Zaki SR: Elucidation of Nipah virus morphogenesis and replication using ultrastructural and molecular approaches. Virus Res 2002, 92:89–98
19. Williamson MM, Hooper PT, Selleck PW, Westbury HA, Slocombe RFS: A guinea-pig model of Hendra virus encephalitis. J Comp Path 2001, 124:273–279
20. Chua KB, Lam SK, Goh KJ, Hooi PS, Ksiazek T, Kamarulzaman A, Olson J, Tan CT: The presence of Nipah virus in respiratory secretions and urine of patients during an outbreak of Nipah virus encephalitis in Malaysia. J Infect 2001, 42:40–43
21. Griffin DE, Bellini WJ: Measles virus. Field's Virology. Edited by B Fields, D Knipe, P Howley, R Chanock, J Melnick, T Monath, B Roizman, S Straus. Philadelphia, Lippincott-Raven, 1996, pp 1267–1312